Supplementary Information for:

Transcription activation mechanism of a non-canonical bacterial DNA damage response pathway

Rajiv R. Singh[1], Amani Chinni[2], Emily Cannistraci[1], Raul Salinas[1], Kevin Gozzi[2] and Maria A. Schumacher[1]

[1]*Department of Biochemistry, 307 Research Dr., Box 3711, Duke University Medical Center, Durham, NC 27710, USA.*

[2]*Rowland Institute at Harvard, 52 Oxford St, Harvard University, Cambridge, MA 02138*

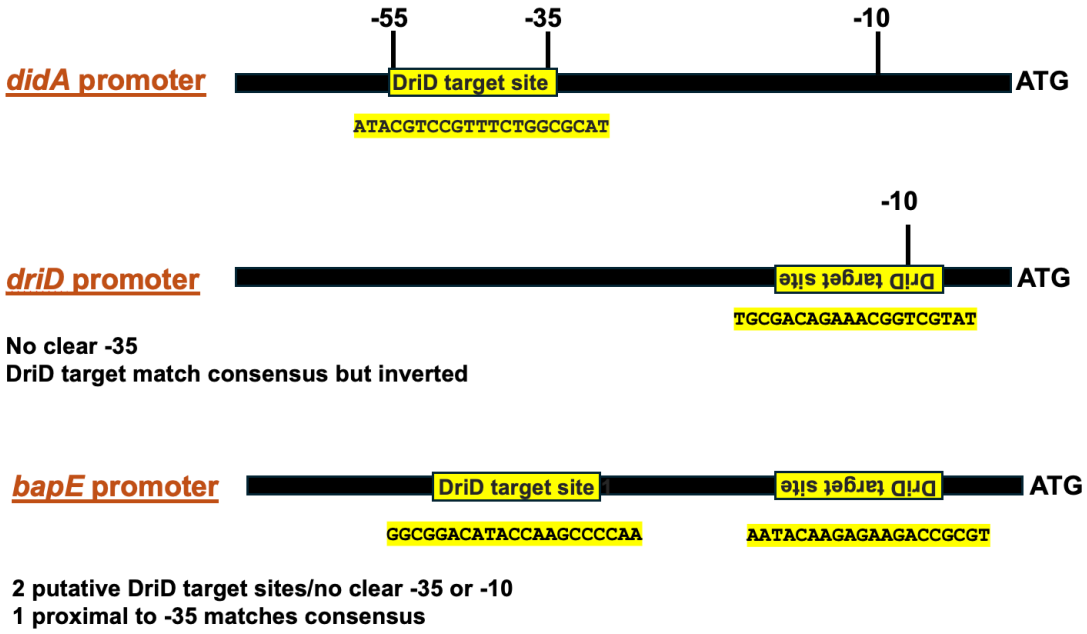

Supplementary Figure 1. Promoters bound by DriD. Shown are schematic diagrams of promoters (*didA, driD* and *bapE*) bound by DriD and utilized for cryo-EM structure determination in this study. Putative DriD target DNA binding sites are boxed and colored yellow with the sequence located beneath each. The transcription starts sites are indicated by ATG and the predicted -35 and other elements are indicated above each promoter.

‘

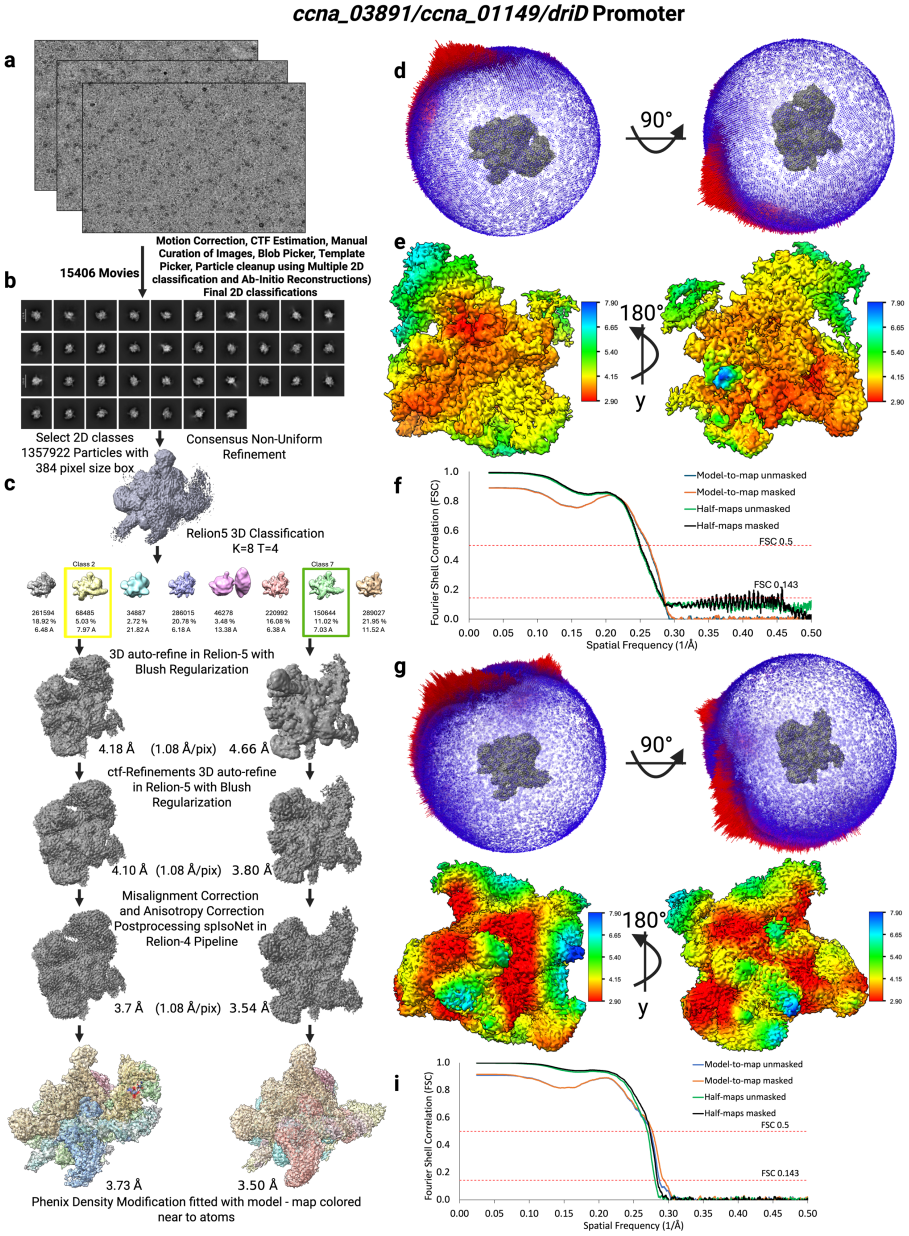

Supplementary Figure 2. Cryo-EM data processing workflow of the DriD-ssDNA-RNAP-σ73-*CCNA_03891/CCNA_01149* promoter and RNAP-σ73-*CCNA_03891/CCNA_01149* promoter structures. (**a**) Representative micrographs. **(b)** A subset of the 2D classes showing clear structural features. **(c)** Flow diagram of the data processing strategy. **(d)** Angular distribution maps of the final particle set used in the reconstruction of *Cc*-DriD-ssDNA-RNAP-σ73-*CCNA_03891/CCNA_01149* (ccna) promoter complex. **(e)** Final map colored by local resolution of the *Cc*-DriD-ssDNA-RNAP-σ73-*CCNA_03891/CCNA_01149* promoter complex between 2.9-7.9Å. (**f**) Masked and unmasked half-map and model FSC curves used to determine global resolution of the *Cc*-DriD-ssDNA-RNAP-σ73-*CCNA_03891/CCNA_01149* (ccna) promoter complex. **(g)** Angular distribution maps of the final particle set used in the reconstruction of the *Cc*-RNAP-σ73-*CCNA* promoter complex. **(h)** Final map colored by local resolution of the *Cc*-RNAP-σ73-*CCNA_03891/CCNA_01149* promoter complex dataset between 2.9-7.9Å. **(i)** Masked and unmasked half-map and model FSC curves used to determine global resolution of the *Cc*-RNAP-σ73-*CCNA_03891/CCNA_01149* promoter complex.

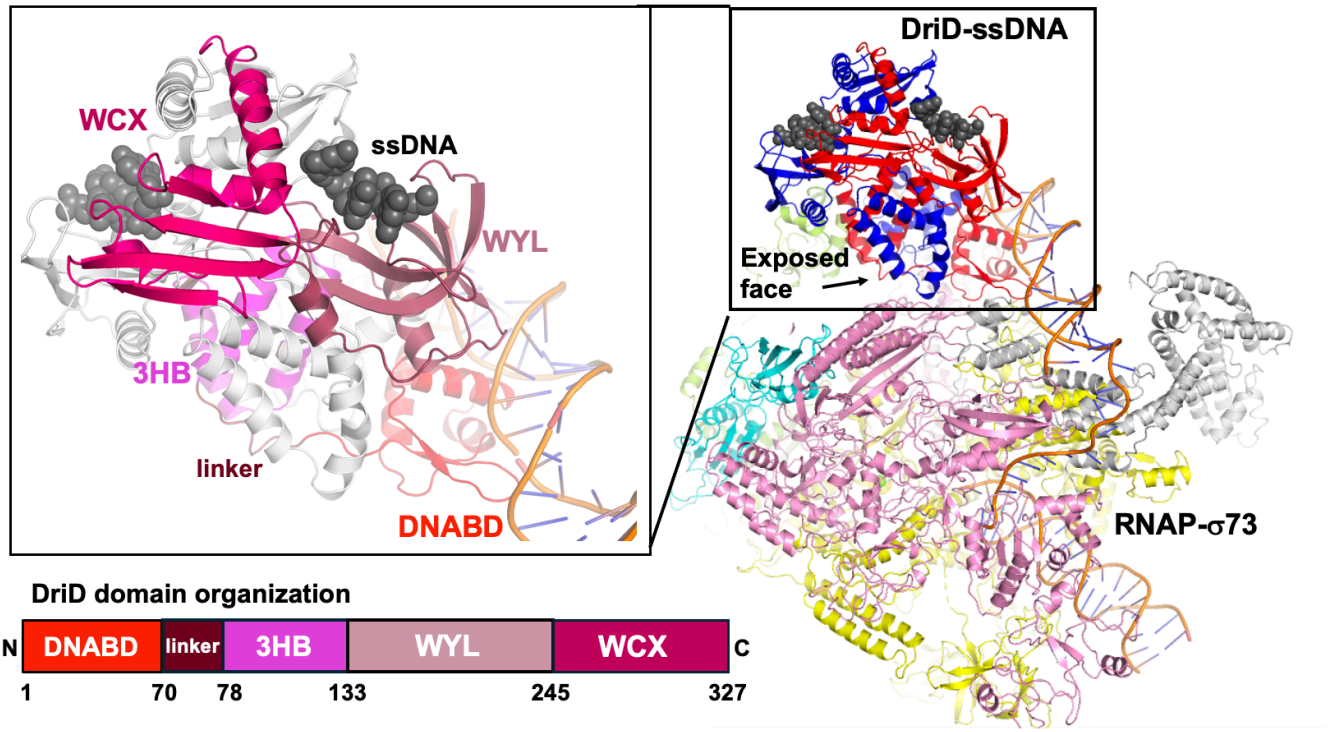

Supplementary Figure 3. Domain organization and asymmetric binding of the DriD-ssDNA dimer to the promoter. Right shows the overview of the DriD-ssDNA-RNAP-σ73-driD promoter complex. To the left is a close-up view showing just DriD-ssDNA with the domains colored as shown in the schematic below. Each domain is also labeled.

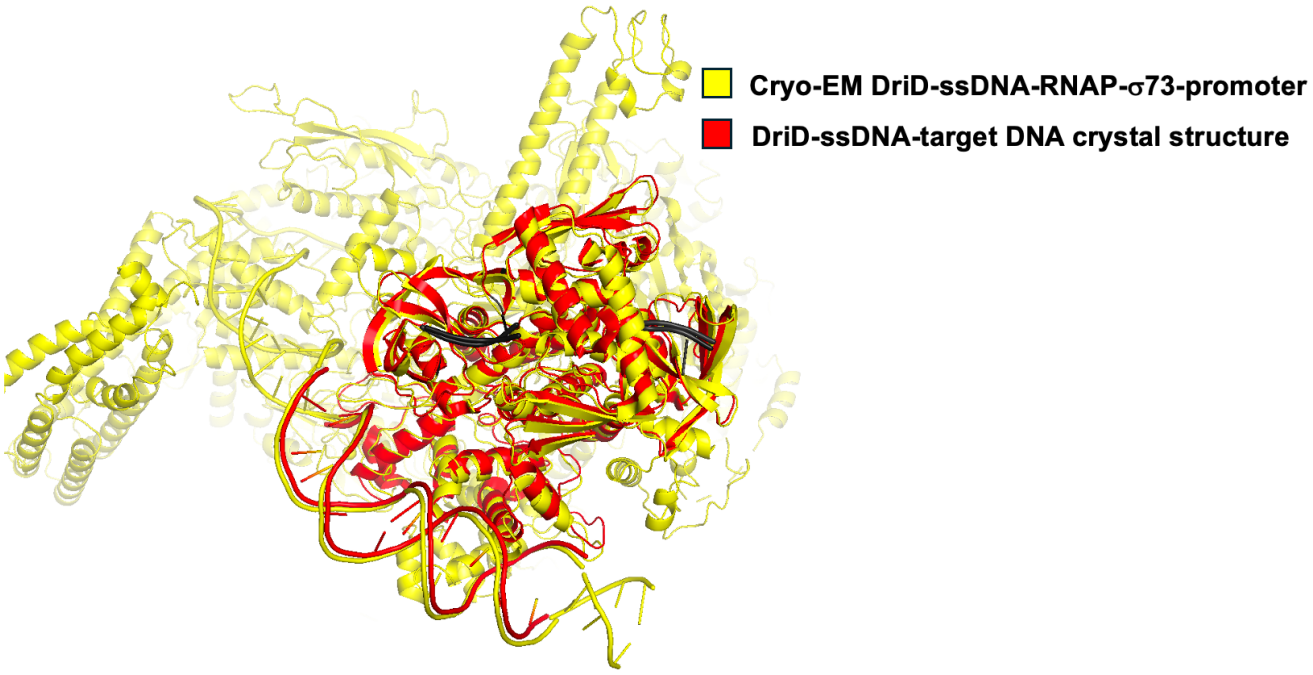

Supplementary Figure 4. Overlay of the DriD-ssDNA-target DNA crystal structure onto promoter-RNAP-bound DriD. In the overlay, the DriD-ssDNA-target DNA crystal structure is red and the cryo-EM DriD-ssDNA-RNAP-σ73-promoter structure is colored yellow.

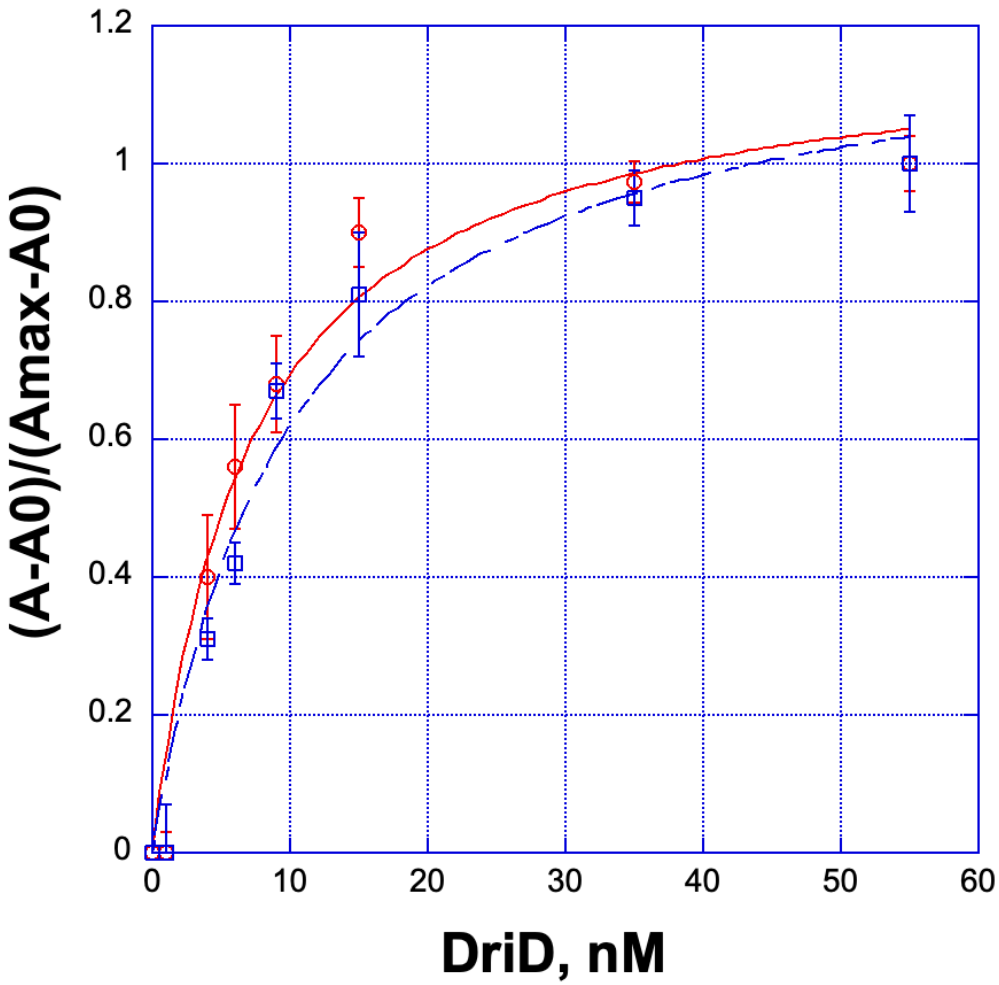

Supplementary Figure 5. FP binding isotherm showing binding of WT DriD (red circles) and DriD(G18K-A20K) (blue squares) in the presence of 100 μM ssDNA binding to target DNA. Three technical replicates were done for each.

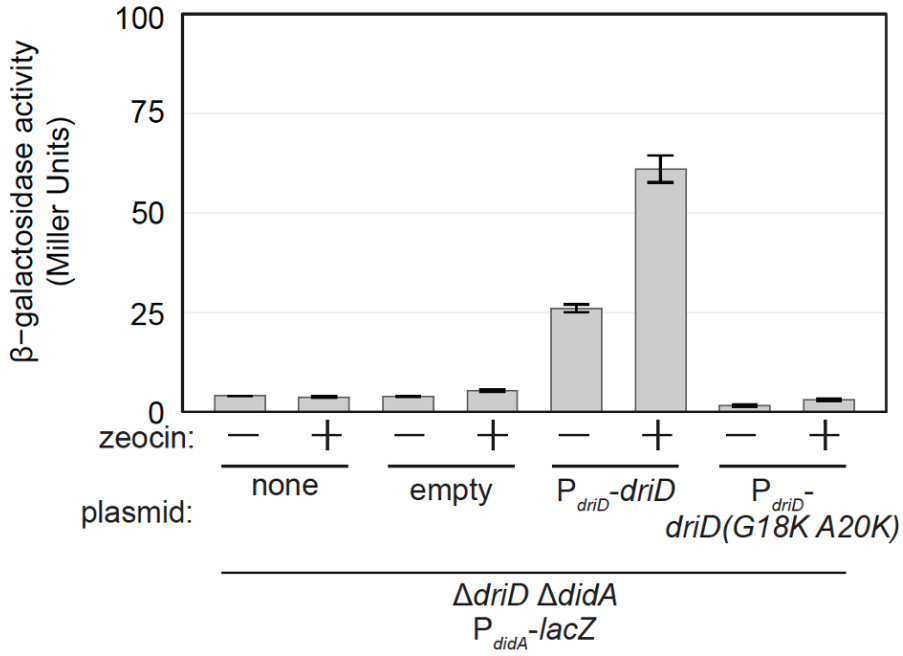

Supplementary Figure 6. β-galactosidase assays of the P_{didA}-*lacZ* as a readout for DriD-mediated transcription activation. Strains bearing a P_{didA}-*lacZ*, a *driD* deletion, and either no plasmid, an empty vector, a wild-type *driD* complementation or the mutant *driD* (G18K-A20K) were treated with zeocin to induce *didA* transcription activation. Mean and standard deviation of three biological replicates are shown.

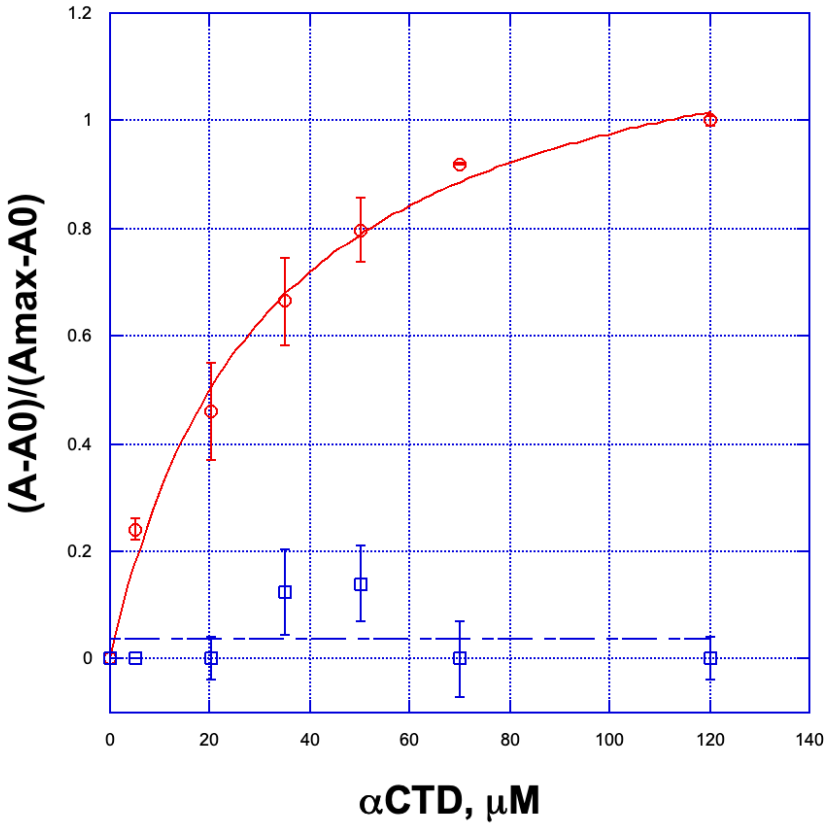

Supplementary Figure 7. FP binding isotherm showing binding of αCTD to WT DriD-ssDNA-target DNA (red circles) and to DriD(R121E-R122E-P125E-E128R)-ssDNA-target DNA (blue squares). Three technical replicates were done for each.

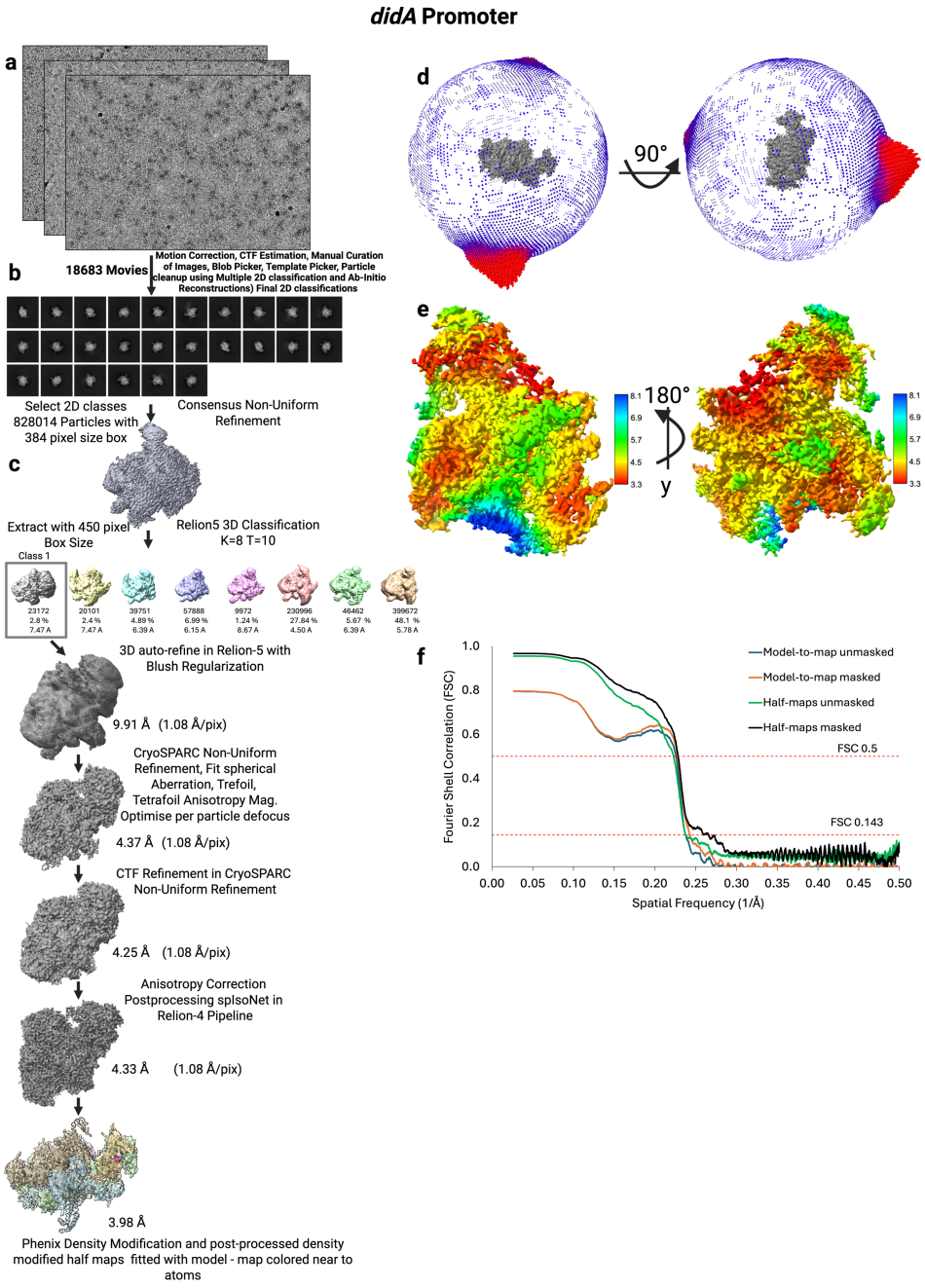

Supplementary Figure 8. Cryo-EM data processing workflow of the DriD-ssDNA-RNAP-σ73-*didA* promoter structure. (**a**) A few representative micrographs. (**b**) A subset of the 2D classes showing clear structural features. (**c**) Flow diagram of the data processing strategy. (**d**) Angular distribution maps of the final particle set used in the reconstruction of *Cc*-DriD-ssDNA-RNAP-σ73-*didA* promoter complex. **(e)** Final map colored by local resolution of *Cc*-DriD-ssDNA-RNAP-σ73-*didA* promoter complex between 3.3-8.1 Å. **(f)** Masked and unmasked half-map and model FSC curves used to determine global resolution.

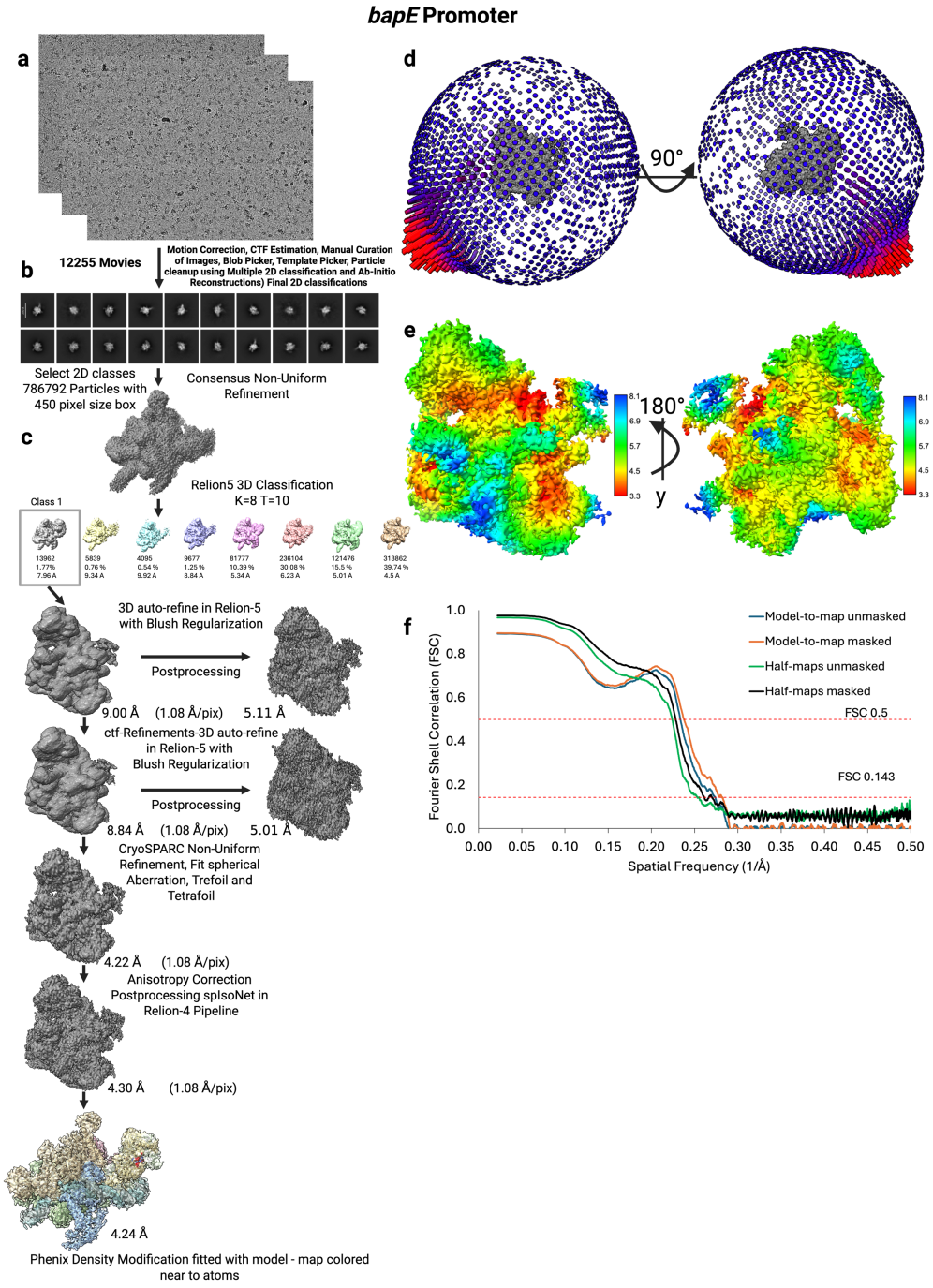

Supplementary Figure 9. Cryo-EM data processing workflow of the DriD-ssDNA-RNAP-σ73-*bapE* promoter structure. (**a**) A few representative micrographs. (**b**) A subset of the 2D classes showing clear structural features. (**c**) Flow diagram of the data processing strategy. (**d**) Angular distribution maps of the final particle set used in the reconstruction of *Cc*-DriD-ssDNA-RNAP-σ73-*bapE* promoter complex. **(e)** Final map colored by local resolution of *Cc*-DriD-ssDNA-RNAP-σ73-*bapE* promoter complex between 3.3-8.1 Å. **(f)** Masked and unmasked half-map and model FSC curves used to determine global resolution.

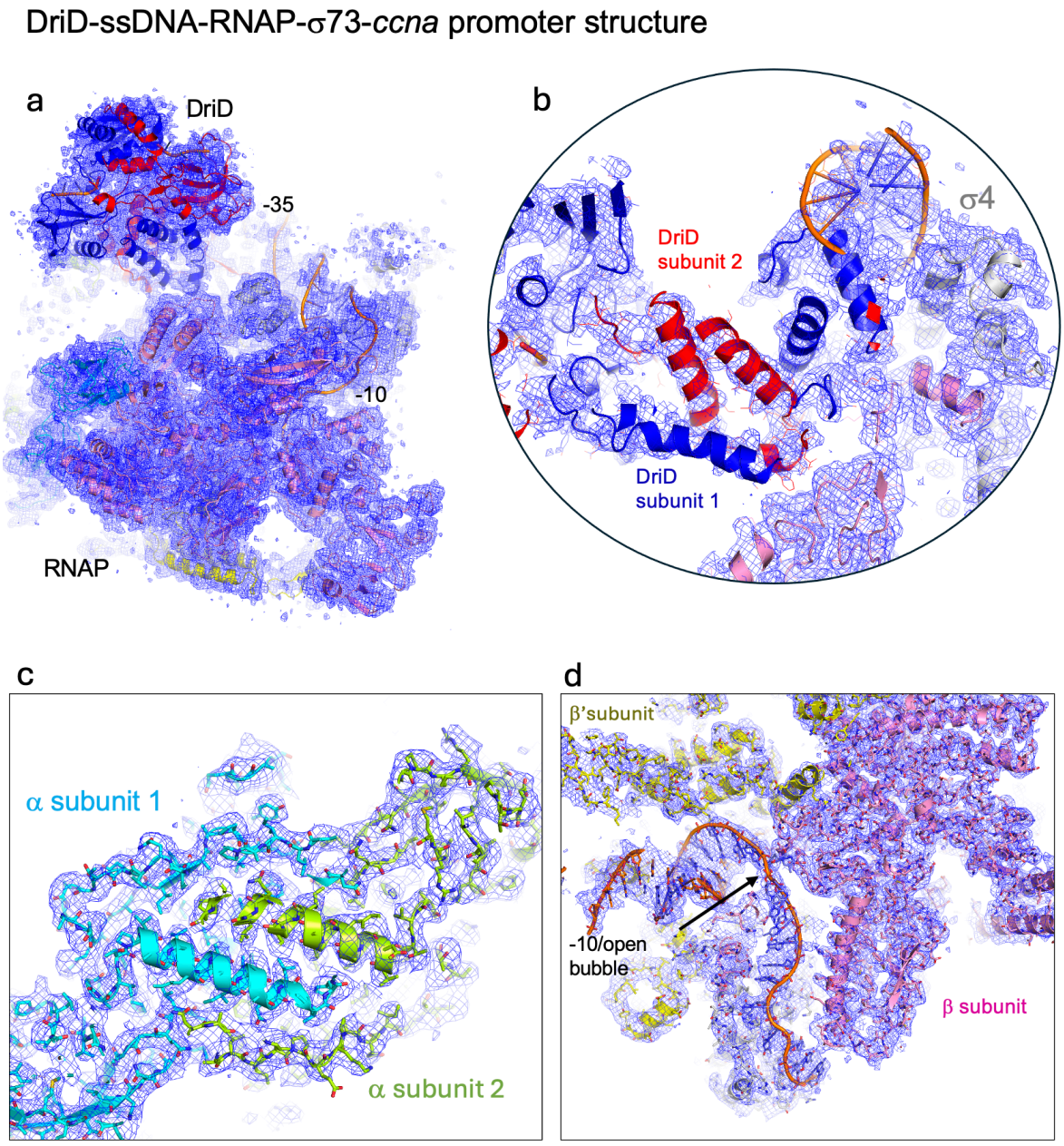

Supplementary Figure 10. Representative densities for the cryo-EM DriD-ssDNA-RNAP-σ73-*CCNA_03891/CCNA_01149* promoter DNA complex. Shown is representative density for various regions of the structure, including the overall structure. (**a**) overall structure with the cryo-EM map included with the structural domains, DriD and DNA colored as in Figure 1 (map contour 1.7 σ). (**b**) Close up of the DriD DNABD region around the DNA and the σ4 domain. (**c**) Close up of the RNAP α subunit dimer region. (**d**) Desnity for the DNA open bubble and the β and β' subunits. Map contour for the two lower figures is 2.4 σ.

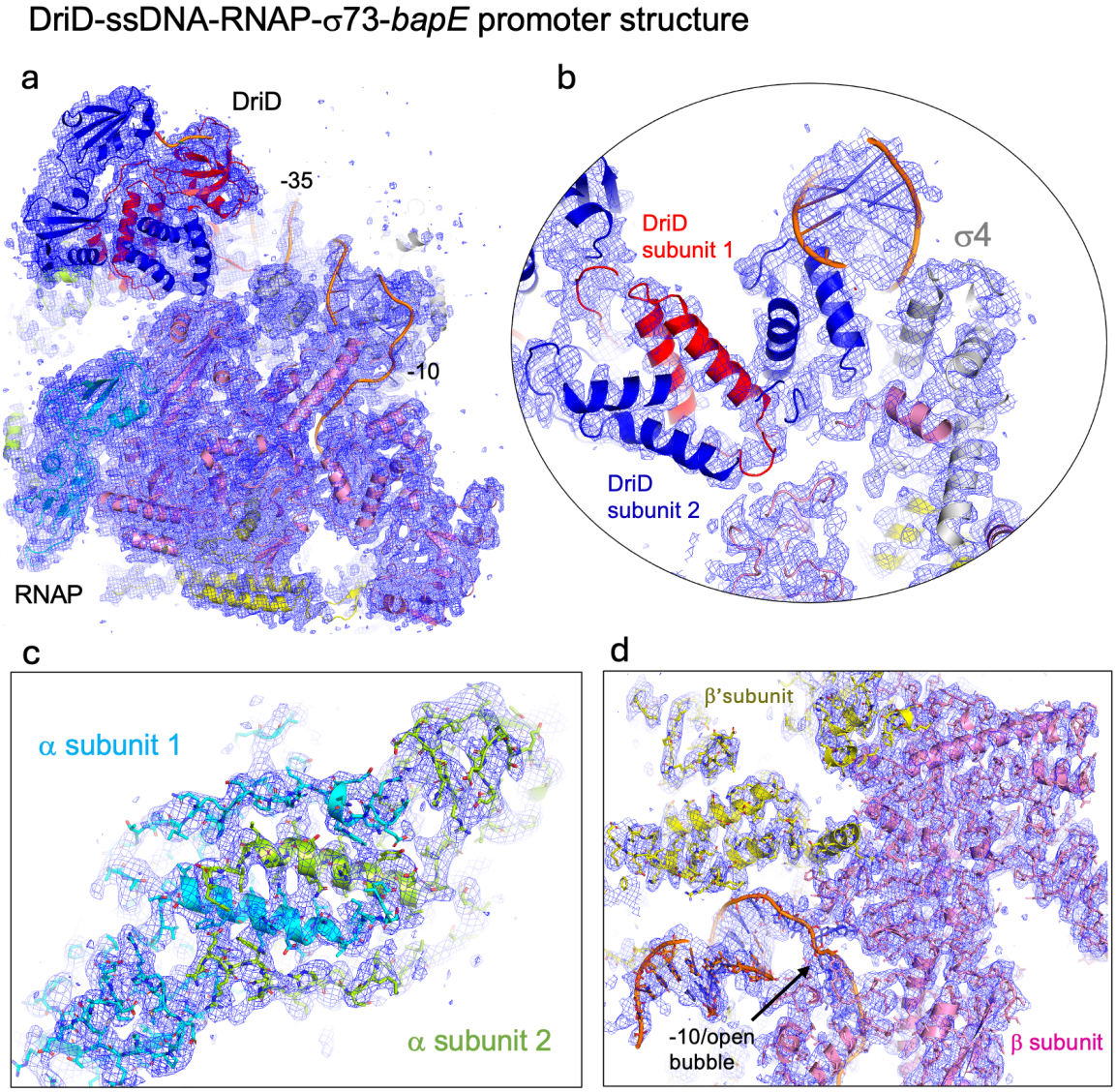

Supplementary Figure 11. Representative densities for the cryo-EM DriD-ssDNA-RNAP-σ73-*bapE* promoter DNA complex. Shown is representative density for various regions of the structure, including the overall structure. (**a**) Overall structure with the cryo-EM map included with the structural domains, DriD and DNA colored as in Figure 4 (b). (**b**) Close up of the DriD DNABD region around the DNA and the σ4 domain. The map contour is 4.7 σ. (**c**) Close up of the RNAP α subunit dimer region. (**d**) Density for the DNA open bubble and the β and β' subunits (map contour 5.2 σ).

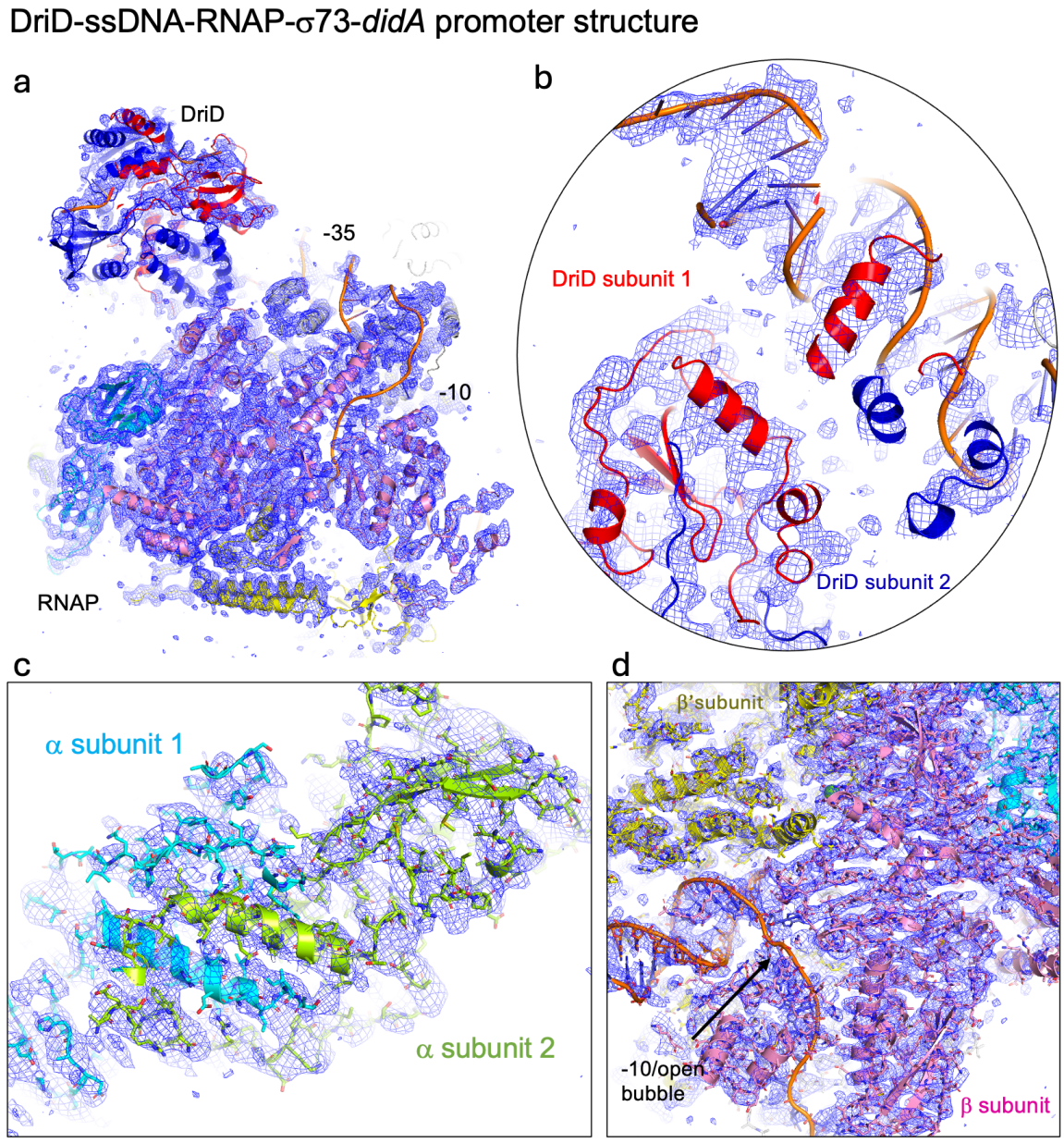

Supplementary Figure 12. Representative densities for the cryo-EM DriD-ssDNA-RNAP-σ73-*didA* promoter DNA complex. Shown is representative density for various regions of the structure, including the overall structure. (**a**) Overall structure with the cryo-EM map included with the structural domains. (**b**) Close up of the DriD DNABD region around the DNA and the σ4 domain. The map contour for the top panels is 4.3 σ. (**c**) Close up of the RNAP α subunit dimer region. (**d**) Density for the DNA open bubble and the β and β' subunits. Map contour of 5.3 σ.

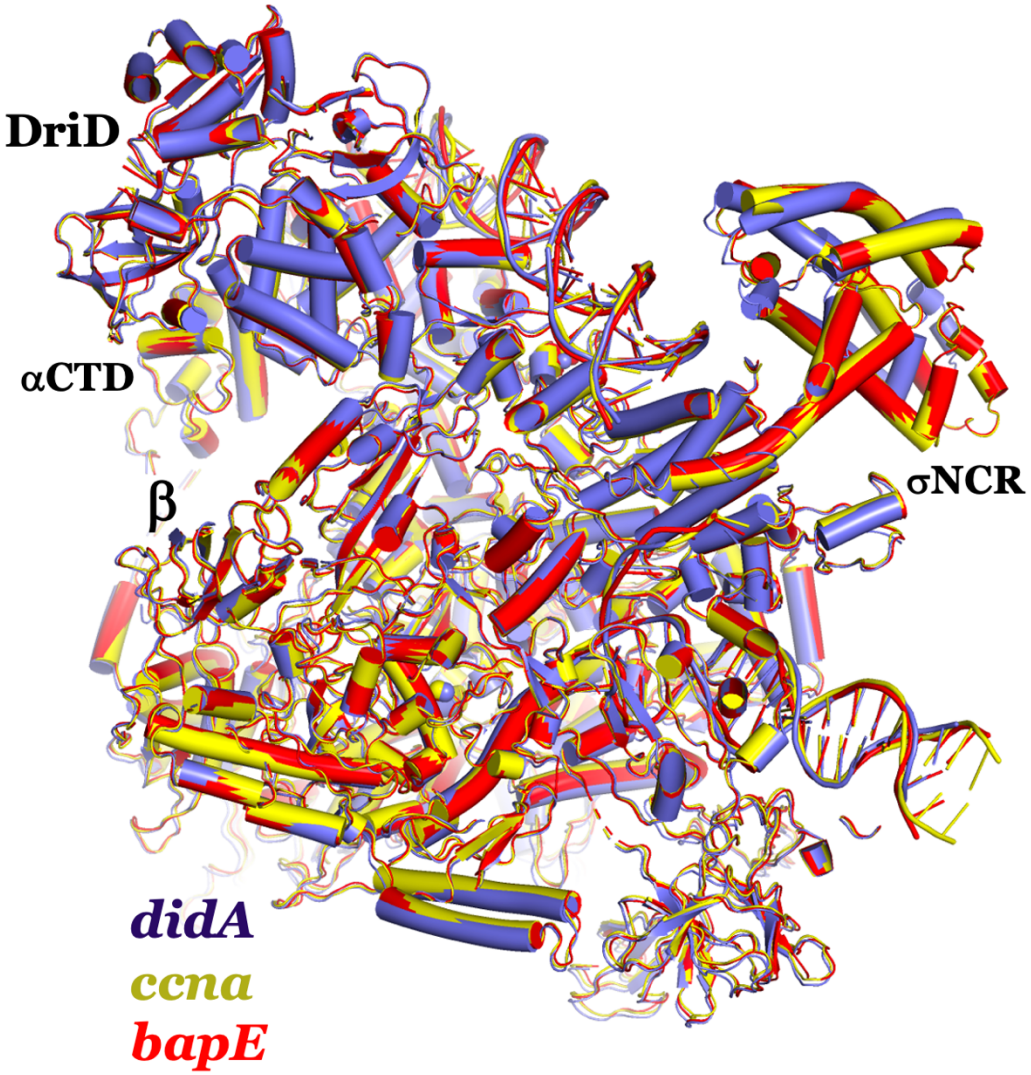

Supplementary Figure 13. Overlay of DriD-ssDNA promoter complexes. Colored in yellow, violet and light_blue are the DriD-ssDNA-RNAP-σ73-*CCNA_03891/CCNA_01149* (*ccna*), DriD-ssDNA-RNAP-σ73-*bapE* and DriD-ssDNA-RNAP-σ73-*didA* promoter complexes, respectively. The complex overlays with rmsds of less than 1.9 Å indicating they are essentially identical in their arrangements.

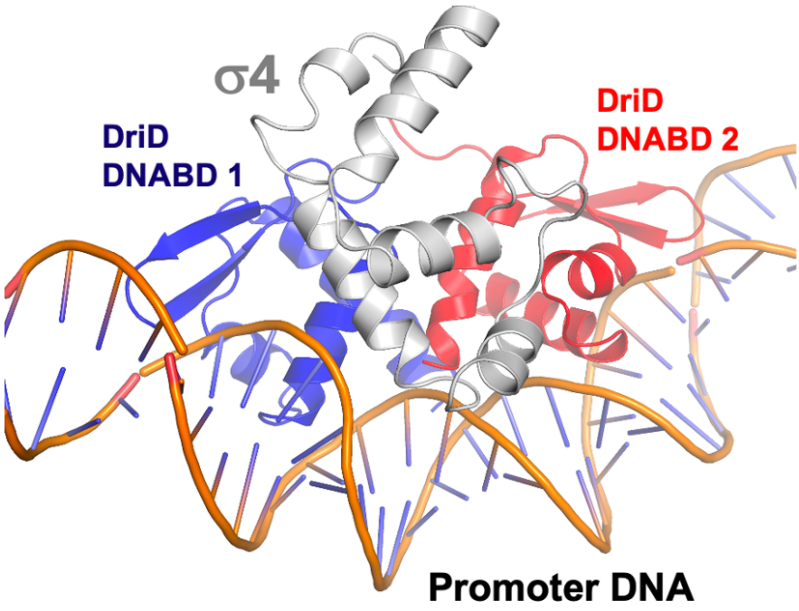

Supplementary Figure 14. The -35 promoter elements in DriD regulated promoters are located at the center of the DriD target DNA binding sites. Shown is a close-up of just the DriD DNABDs, colored blue and red and labeled, bound to the *CCNA_03891/CCNA_01149* promoter with the σ4 domain, colored grey, included. Notably, the DriD DNABDs sandwich the bound σ4 domain, which docks onto the -35 element.

‘

Supplementary Table 1. Cryo-EM analyses and structure statistics

Cryo-EM data collection, refinement, and validation statistics.				
	DriD-ssDNA-RNAP-σ73-driD/ccna promoter	***RNAP-σ73-driD/ccna promoter***	***DriD-ssDNA-RNAP-σ73-didA promoter***	***DriD-ssDNA-RNAP-σ73-bapE promoter***
	PDB: 9PFV	**PDB: 9PGH**	**PDB: 9PGA**	**PDB: 9PFQ**
	EMD-71615	**EMD-71632**	**EMD-71624**	**EMD-71610**
Data collection and Processing				
Electron microscope	**Titan Krios (Duke)**	**Titan Krios (Duke)**	**Titan Krios (Duke)**	**Titan Krios (Duke)**
Detector	**K3**	**K3**	**K3**	**K3**
Magnification	**81,000x**	**81,000x**	**81,000x**	**81,000x**
Voltage (keV)	**300**	**300**	**300**	**300**
Electron exposure (e-/Å^2)	**58.7**	**58.7**	**56.6**	**59**
Number of frames per movie	**60**	**60**	**60**	**60**
Defocus range (μm)	**-0.8 to -2.5**	**-0.8 to -2.5**	**-0.8 to -2.5**	**-0.8 to -2.5**
Pixel size (Å)	**1.08**	**1.08**	**1.08**	**1.08**
Initial micrographs	**15406**	**15406**	**18683**	**12255**
Final micrographs	**14781**	**14781**	**16387**	**11122**
Total extracted particles (no.)	**2,373,048**	**2,373,048**	**2,019,352**	**811,774**
Refined particles (no.)	**1,357,922**	**1,357,922**	**828,014**	**807,385**
Reconstruction				
Final particles (no.)	**68,485**	**150,644**	**23,172**	**13,962**
Box size (unbinned) (pixels)	**384**	**384**	**450**	**450**
Symmetry imposed	**C1**	**C1**	**C1**	**C1**
FSC 0.143 (unmasked/masked) (Å)	**4.41/4.10**	**4.41/3.77**	**4.31/4.22**	**4.46/4.22**
Map sharpening B-factor (Å^2)	**-75.86**	**-97.37**	**-35.4**	**-31**
spIsoNet Misalignment and Anisotropy Correction				
FSC 0.143 (masked) (Å)	**3.7**	**3.54**	**4.33**	**4.3**
Map sharpening B-factor (Å^2)	**-59.11**	**-70.45**	**-35.4**	**-31**
Phenix Density Modification (Å)	**3.7**	**NA**	**3.98**	**4.24**
Refinement				
Model composition				
Non-hydrogen atoms	**36,328**	**30,040**	**35,717**	**36,042**
Protein residues	**4,461**	**3,718**	**4,425**	**4,453**
Nucleotides	**125**	**97**	**121**	**121**
Ions/Ligands	**3**	**3**	**3**	**3**
MolProbity score	**1.97**	**1.99**	**2.22**	**2.02**
Clash score	**9.38**	**10.3**	**15.19**	**10.68**
Bonds (RMSD)				
Bond lengths (Å)	**0.003**	**0.004**	**0.004**	**0.004**
Bond angles (°)	**0.556**	**0.658**	**0.677**	**0.697**
Ramachandran plot (%)				
Favored (%)	**92.31**	**92.75**	**90.49**	**92.16**
Allowed (%)	**7.69**	**7.25**	**9.51**	**7.79**
Disallowed (%)	**0.00**	**0.00**	**0.00**	**0.05**
Foot Note: NA-Not applicable; RNAP-σ73-driD/ccna promoter complex was not density modified.				

Supplementary Table 2. Strains used in this study

Strains	Description	Source
ML76	CB15N wild-type	1
ML77	CB15N *rec526*	2
ML3757	CB15N Δ*driD*::*tet*^{R}	3
ML3760	CB15N pRVMCS-2(*kan*^{R})::P$_{driD}$-*driD*; Δ*driD*::*tet*^{R}, Δ*didA*, *hfaB*::P$_{didA}$-*lacZ*	3
KG570	CB15N Δ*driD*::*tet*^{R}, Δ*didA*, *hfaB*::P$_{didA}$-*lacZ*	4
ML2174	CB15N Δ*driD*	5
KG720	CB15N *hfaB*::P$_{didA}$-*lacZ*	This study
KG721	CB15N Δ*driD*, *hfaB*::P$_{didA}$-*lacZ*	This study
KG722	CB15N Δ*driD*, *hfaB*::P$_{didA}$-*lacZ*, pRVMCS-2 (empty)	This study
KG723	CB15N Δ*driD*, *hfaB*::P$_{didA}$-*lacZ*, pRVMCS-2::P$_{driD}$-*driD*	This study
KG724	CB15N *hfaB*::P$_{03891/01149}$-*lacZ*	This study
KG725	CB15N Δ*driD*, *hfaB*::P$_{03891/01149}$-*lacZ*	This study
KG726	CB15N Δ*driD*, *hfaB*::P$_{03891/01149}$-*lacZ*, pRVMCS-2 (empty)	This study
KG727	CB15N Δ*driD*, *hfaB*::P$_{03891/01149}$-*lacZ*, pRVMCS-2::P$_{driD}$-*driD*	This study
KG728	CB15N *hfaB*::P$_{driD}$-*lacZ*	This study
KG729	CB15N Δ*driD*, *hfaB*::P$_{driD}$-*lacZ*	This study
KG730	CB15N Δ*driD*, *hfaB*::P$_{driD}$-*lacZ*, pRVMCS-2 (empty)	This study
KG731	CB15N Δ*driD*, *hfaB*::P$_{driD}$-*lacZ*, pRVMCS-2::P$_{driD}$-*driD*	This study
KG732	CB15N Δ*driD*::*tet*^{R}, Δ*didA*, *hfaB*::P$_{didA}$-*lacZ*, pRVMCS-2::P$_{driD}$-*driD* (G18K A20K)	This study
KG733	CB15N Δ*driD*::*tet*^{R}, Δ*didA*, *hfaB*::P$_{didA}$-*lacZ*, pRVMCS-2::P$_{driD}$-*driD**	This study

Supplementary Table 3. Plasmids used in this study

Plasmids	**Description**	**Source**
pRVMCS-2 (empty)	low-copy vector bearing inducible promoter and *kan*^{R}	6
pNPTS138	used to create genome modifications via homologous recombination	6
pNPTS138-*hfaB*::*lacZ*	pNPTS138 bearing lacZ flanked by *hfaB* upstream and downstream homology regions	This study
pRVMCS-2:: P$_{driD}$-*driD*	pRVMCS-2 with P$_{driD}$-*driD* at SacI/SacII	3
pRVMCS-2:: P$_{driD}$-*driD* (G18K A20K)	pRVMCS-2 with P$_{driD}$-*driD* (G18K A20K) at SacI/SacII	This study
pNPTS138-*hfaB*::P$_{didA}$-*lacZ*	pNPTS138 bearing *hfaB*-P$_{didA}$-lacZ-*hfaB*	This study
pNPTS138-*hfaB*::P$_{driD}$-*lacZ*	pNPTS138 bearing *hfaB*-P$_{driD}$-*lacZ-hfaB*	This study
pNPTS138-*hfaB*::P$_{03891/01149}$-*lacZ*	pNPTS138 bearing *hfaB*-P$_{03891/01149}$-*lacZ-hfaB*	This study

Supplementary Table 4. Oligonucleotides used in this study

Oligonucleotides	**Sequence**
qRT-PCR of *rpoA*	
oKRG360	ACATCGTCTACATCGGCGAC
oKRG361	GGCGAGCACTTCCTTGATCT
qRT-PCR of *driD*	
oKRG322	ACCTGAAGGTGCTCGACAAG
oKRG323	GTCGTGATAGATGCCGAAGC
qRT-PCR of *didA*	
oKRG356	GCTCATGCTGTTCGTGGTC
oKRG357	CTACCAGCCCCAGTGACG
qRT-PCR of *CCNA_03891*	
oKRG723	CTTCGCCGACATCCATCGC
oKRG724	GGTGACGCGGACGATCTG
qRT-PCR of *CCNA_01149*	
oKRG717	CGGTCAGCAACGCCGTCAAC
oKRG718	GAGGCCGTAACCGGTCAGG
Cloning of *hfaB* UHR (627/628), DHR (629/630) and *lacZ* (802/803) into pNPTS138 to make pNPTS138-*hfaB*::*lacZ*	
oKRG627	cagcagCTTAAGTGTCCTGGTTCGACGTCACAGC
oKRG628	cagcagGTCGACACACCGACGGCCTGAAGGG
oKRG629	cagcagAAGCTTGGATGTTGTAGTTCAGCTCGGTGATGC
oKRG630	cagcagACTAGTAACAATACCGTCATCGTCAATTCCAGCC
oKRG802	gatcgtcgacATGACCATGATTACGGAT
oKRG803	tactacAAGCTTTTATTTTTGACACCAGACCAACTG
Cloning of *didA* promoter to make pNPTS138-*hfaB*::P$_{didA}$-*lacZ*	
oKRG783	cagcaggtcgacGGTGATCGTCTGGCCCATGG
oKRG784	cagcagggatccTCTCCTTcCcctcatctgatggaagcgacc
Cloning of *driD* promoter to make pNPTS138-*hfaB*::P$_{driD}$-*lacZ*	
oKRG785	cagcaggtcgacCGAAGGTCCTTGGGTTCTCCAG
oKRG786	cagcagggatccTCTCCTTcTCATACGACCGTTTCTGTCGC
Cloning of *CCNA_03891/01149* promoter to make pNPTS138-*hfaB*::P$_{03891/01149}$-*lacZ*	
oKRG799	cagcaggtcgacGccgcccgtcATACGACC
oKRG800	cagcagggatccTCTCCTTcCttgggttctccAGGGGTGATG
PCR of *driD* for fusion cloning	

oKRG316	GATCCCGCGGTTCATGCCCTGGCTCCTACCAC
oKRG317	GATCGAGCTCGTCAGGCGCAGAGACGCAGGGGTTC
Cloning of pRVMCS-2::P*driD*-*driD* (G18K A20K)	
oKRG797	GCTGGCTAAGTCCAAAGAGGGGCTG
oKRG798	CAGCCCCTCTTTGGACTTAGCCAGC

Supplementary References

1. Evinger, M. & Agabian, N. (1977) Envelope-associated nucleoid from *Caulobacter crescentus* stalked and swarmer cells. *J. Bacteriol*. **132**, 294-301 (1977).

2. O'Neill, E.A., Hynes R.H. & Bender R.A. (1985) Recombination deficient mutant of *Caulobacter crescentus*. *Mol. Gen. Genet.* **198**, 275-278 (1985).

3. Gozzi, K., Salinas, R., Nguyen, V.D., Laub, M.T. & Schumacher, M. ssDNA is an allosteric regulator of the *C. crescentus* SOS-independent DNA damage response transcription activator, DriD. *Genes & Dev*. **36**, 618-633 (2022).

4. Schumacher, M.A., Cannistraci E., Salinas, R., Lloyd, D., Messner, E. & Gozzi, K. Structure of the WYL-domain containing transcription activator, DriD, in complex with ssDNA effector and DNA target site. *Nucleic Acids Res.* **52**, 1435-1449 (2023).

5. Modell, J.W., Kambara, T.K., Perchuck, B.S. & Laub, M.T. A DNA damage-induced, SOS-independent checkpoint regulates cell division in *Caulobacter crescentus*. *PLoS Biol.* **12**, e1001977 (2014).

6. Thanbichler, M., Iniesta, A.A. & Shapiro, L. A comprehensive set of plasmids for vanillate- and xylose- inducible gene expression in *Caulobacter crescentus*. *Nucleic Acids Res.* **35**, 3137 (2007).